ISSN 1070-3284, Russian Journal of Coordination Chemistry, 2014, Vol. 40, No. 7, pp. 495–504. © Pleiades Publishing, Ltd., 2014.
Original Russian Text © P.S. Koroteev, Zh.V. Dobrokhotova, N.N. Efimov, A.B. Ilyukhin, V.M. Novotortsev, 2014, published in Koordinatsionnaya Khimiya, 2014, Vol. 40, No. 7, pp. 438–448.

Dedicated to the 80th Anniversary of the Kurnakov Institute of General and Inorganic Chemistry

New Binuclear Ferrocenecarboxylates of Rare-Earth Metals as Precursors for Ferrites: Syntheses, Structures, and Solid-Phase Thermolysis

P. S. Koroteev*, Zh. V. Dobrokhotova, N. N. Efimov, A. B. Ilyukhin, and V. M. Novotortsev

Kurnakov Institute of General and Inorganic Chemistry, Russian Academy of Sciences, Leninskii pr. 31, Moscow, 119991 Russia

**e-mail: pskoroteev@list.ru*

Received December 5, 2013

Abstract—New ferrocenecarboxylates of rare-earth metals, $[Ln_2(\mu\text{-}O,\eta^2\text{-}OOCFc)_2(\mu_2\text{-}O,O'\text{-}OOCFc)_2(\eta^2\text{-}NO_3)_2(DMSO)_4]$ (Ln = Gd (**I**), Tb (**II**), and Y (**III**)) and $[Gd_2(\mu\text{-}O,\eta^2\text{-}OOCFc)_2(\eta^2\text{-}OOCFc)_4(DMSO)_2(H_2O)_2] \cdot 2DMSO \cdot 2CH_2Cl_2$ (**IV**), are synthesized and characterized by X-ray diffraction analysis. Unlike all earlier known ferrocenecarboxylates of rare-earth metals, in isostructural compounds **I**–**III** the Ln atoms are linked by four bridging carboxyl residues, two of which are chelate-bridging (the coordination number of Ln is 9). Binuclear structure **IV** is formed by two chelate-bridging carboxylate ligands (the coordination number of Gd is 9). Weak antiferromagnetic and weak ferromagnetic interactions between the Gd atoms are observed in complexes **I** and **IV**, respectively. The thermal decomposition of the synthesized compounds is studied by differential scanning calorimetry and thermogravimetry. According to the X-ray diffraction data, the final thermolysis products of the complexes in air are garnets $Ln_3Fe_5O_{12}$.

DOI: 10.1134/S1070328414070045

INTRODUCTION

One of important trends in investigation of modern chemistry relating the coordination chemistry and materials science is the study of possibilities of using coordination compounds as molecular precursors for the directed synthesis of various inorganic materials of certain composition and structure. The synthesis of mixed oxide systems using heterometallic coordination compounds from which the desired oxide would be formed after the removal of the organic moiety of the molecule, under relatively mild conditions, is of interest, because the composition of the expected oxide and, possibly, its properties can be programmed, in principle, already at the level of the molecular precursor. In particular, possibilities of preparing various complex oxide materials from organometallic complexes were discussed: multiferroics [1], semiconductor nanoparticles [2], polyfunctional [3] and segnetoelectric [4] thin films, and multiferroic manganites $LnMn_2O_5$ [5]. Studies of heterometallic complexes containing 3*d* and 4*f* elements are intensely developing presently. Numerous diverse heterometallic 3*d*–4*f* complexes in which metal ions are linked by polydentate ligands (carboxylates, β-diketonates, Schiff bases, and amino alcohols) are known and were studied [6–9]. Ferrocene discovered in the middle of the last century has a lot of many interesting properties and is a potential building block for heterometallic complexes. Organometallic compounds containing Fe in the ferrocene fragment and the second metal in the ionic form represent a unique type of heterometallic complexes, since they are capable of combining specific properties of ferrocene with the properties of the second metal ion [10, 11]. Heterometallic 3*d*–3*d* carboxylates of this type have first been synthesized more than twenty five years ago: many complexes of this kind are known and were studied in detail [12, 13]. Heterometallic 3*d*–4*f* carboxylates containing the ferrocene fragment that were synthesized within the last decade are less studied. Only a series of rare-earth metal complexes with ferrocenecarboxylic [12, 14, 15], *p*-ferrocenylbenzoic [16], and β-ferrocenoylpropionic [17] acids are known. The ability of rare-earth metal ferrocenecarboxylates to serve as precursors for practically important mixed-oxide functional materials, such as lanthanide–iron garnets and perovskite-like ferrites remained yet unstudied. The purpose of this work is to synthesize new ferrocenecarboxylate rare-earth metal complexes and to study their physicochemical properties and solid-phase thermolysis.

EXPERIMENTAL

The following commercial reagents were used for the synthesis: hydrated lanthanide nitrates $Ln(NO_3)_3 \cdot 6H_2O$ and $GdCl_3 \cdot 6H_2O$ (Alfa Aesar), ferrocenecarboxylic acid (Aldrich), and solvents MeOH, DMSO, n-C_6H_{14}, and C_6H_5Me (Alfa Aesar). Prior to use methanol was distilled over magnesium, DMSO was distilled in vacuo, and hexane and toluene were successively distilled over P_2O_5 and over sodium. IR spectra were recorded in the range from 400 to 4000 cm^{-1} on a Spectrum-65 PerkinElmer FT-IR spectrometer in KBr pellets. Microanalyses were performed on a Euro Vector Element Analyser (Model EA 3000) CHN analyzer.

Synthesis of $[Ln_2(\mu\text{-}O,\eta^2\text{-}OOCFc)_2(\mu_2\text{-}O,O'\text{-}OOCFc)_2(\eta^2\text{-}NO_3)_2(DMSO)_4]$ (Ln = Gd (I), Tb (II), Y (III)). Potassium hydroxide (67 mg, 1.20 mmol) was added to a solution of FcCOOH (272 mg, 1.20 mmol) in methanol (4 mL). The mixture was stirred for 15 min at room temperature. Then a solution of $Ln(NO_3)_3 \cdot 6H_2O$ (0.6 mmol) in a mixture of methanol (4 mL) and DMSO (1 mL) was added with stirring. The mixture was stirred for 24 h at room temperature in an argon atmosphere. Then methanol was removed in a vacuum of a water-jet pump. The residue was treated with a hot (~100°C) mixture of toluene (20 mL) and DMSO (1 mL). The solution was filtered in vacuo through a glass filter, and hexane (3–4 mL) was added with stirring. Dark red crystals suitable for X-ray diffraction analysis were formed during several days after the slow cooling of the solution to room temperature in the dark. The yield was 45–55%. An additional amount of the product can be extracted by the successive addition of DMSO (2 mL), hot toluene (20 mL), and hexane (3 mL) to the residue after filtration with intensive stirring. The product precipitates after the filtration and cooling of the solution (total yield up to 75%).

For $C_{52}H_{60}N_2O_{18}S_4Fe_4Gd_2$ (**I**)			
anal. calcd., %:	C, 37.46;	H, 3.63;	N, 1.68.
Found, %:	C, 37.50;	H, 3.61;	N, 1.66.

IR for **I** (KBr, ν, cm^{-1}): 3109 w, 3003 w, 2919 w, 1600 s, 1525 m, 1483 s, 1390 s, 1359 s, 1348 m, 1323 s, 1304 s, 1222 w, 1198 m, 1105 m, 1025 s, 1010 s, 962 m, 934 w, 818 s, 804 m, 794 m, 775 m, 738 w, 718 w, 710 w, 577 m, 507 s, 503 s, 486 m, 452 w, 415 w, 406 w.

For $C_{52}H_{60}N_2O_{18}S_4Fe_4Tb_2$ (**II**)			
anal. calcd., %:	C, 37.39;	H, 3.62;	N, 1.68.
Found, %:	C, 37.41;	H, 3.58;	N, 1.64.

IR for **II** (KBr, ν, cm^{-1}): 3109 w, 3003 w, 2919 w, 1603 s, 1526 m, 1483 s, 1390 s, 1359 s, 1348 m, 1322 s, 1305 s, 1217 w, 1194 m, 1105 m, 1025 s, 1010 s, 962 m, 934 w, 818 s, 803 m, 793 m, 775 m, 738 w, 718 w, 710 w, 577 m, 507 m, 502 m, 486 m, 452 w, 407 w.

For $C_{52}H_{60}N_2O_{18}S_4Fe_4Y_2$ (**III**)			
anal. calcd., %:	C, 40.81;	H, 3.95;	N, 1.83.
Found, %:	C, 40.87;	H, 3.92;	N, 1.79.

IR for **III** (KBr, ν, cm^{-1}): 3109 w, 3003 w, 2920 w, 1612 s, 1530 m, 1485 s, 1391 s, 1360 s, 1348 m, 1323 s, 1306 s, 1222 w, 1198 m, 1106 m, 1025 s, 1010 s, 963 m, 934 w, 817 s, 803 m, 794 m, 776 m, 739 w, 718 w, 710 w, 578 w, 508 s, 501 s, 487 m, 454 w, 411 w.

Synthesis of $[Gd_2(\mu\text{-}O,\eta^2\text{-}OOCFc)_2(\eta^2\text{-}OOCFc)_4(DMSO)_2(H_2O)_2] \cdot 2DMSO \cdot 2CH_2Cl_2$ (IV). Potassium hydroxide (45 mg, 0.8 mmol) was added to a solution of FcCOOH (185 mg, 0.8 mmol) in methanol (4 mL). The solution was stirred for 15 min at room temperature. Then a solution of $GdCl_3 \cdot 6H_2O$ (100 mg, 0.27 mmol) in a mixture of methanol (3 mL) and DMSO (1 mL) was added with stirring. The mixture was stirred for 24 h at room temperature in an argon atmosphere. Methanol was evaporated in a vacuum of a water-jet pump. The residue was treated with a hot (~100°C) mixture of toluene (20 mL) and DMSO (1 mL), and CH_2Cl_2 (3 mL) was added with stirring after cooling to 40°C. The solution was filtered in vacuo through a glass filter, and hexane (3 mL) was added. The mixture was kept for 24 h at room temperature in the dark and cooled to 4°C. Under these conditions, dark red crystals suitable for X-ray diffraction analysis were formed. The yield was 47%. An additional amount of the product can be extracted by the repeated extraction of the residue after filtration with a mixture of solvents of the above indicated composition. The product precipitates after the filtration and cooling of the solution (total yield up to 70%). Crystals of **IV** easily lose solvate CH_2Cl_2 in air at room temperature.

For $C_{76}H_{86}O_{18}S_4Cl_4Fe_6Gd_2$		
anal. calcd., %:	C, 41.36;	H, 3.93.
Found, %:	C, 41.43;	H, 3.96.

IR for **IV** (KBr, ν, cm^{-1}): 3103 w, 3001 w, 1557 s, 1537 s, 1487 s, 1393 s, 1360 s, 1262 w, 1104 w, 1050 w, 1024 m, 1006 m, 956 w, 846 w, 811 m, 799 m, 734 w, 705 w, 553 w, 510 m, 490 m, 408 w.

Magnetic measurements were carried out on an MPMSXL SQUID magnetometer (Quantum Design) in the range from 2 to 300 K in a magnetic field of 5 kOe. Paramagnetic components of magnetic susceptibility (χ_M) were determined taking into account the diamagnetic contribution calculated from Pascal's constants. The effective magnetic moment (μ_{eff}) was calculated by the formula $\mu_{eff} = [(3k/N\beta^2)\chi T]^{1/2} \approx (8\chi T)^{1/2}$, where N is Avogardro's number, k is the Boltzmann constant, and β is Bohr's magneton.

Table 1. Main crystallographic data and experimental conditions for compounds **I**–**IV**

Parameter	Value			
	I	**II**	**III**	**IV**
Crystal system	Triclinic	Triclinic	Triclinic	Triclinic
a, Å	11.0918(4)	11.0892(3)	11.0759(6)	11.8607(17)
b, Å	12.5715(5)	12.5629(3)	12.5533(7)	12.4152(19)
c, Å	13.3376(5)	13.3230(3)	13.2817(7)	16.339(2)
α, deg	63.7087(5)	63.6770(10)	63.6780(10)	78.823(3)
β, deg	89.1549(6)	89.1400(10)	89.2190(10)	75.660(3)
γ, deg	65.8469(5)	65.9450(10)	65.8720(10)	62.327(3)
Space group	$P\bar{1}$	$P\bar{1}$	$P\bar{1}$	$P\bar{1}$
V, Å^3	1489.60(10)	1487.65(6)	1478.54(14)	2055.6(5)
Z	1	1	1	1
Temperature, K	296	293	296	295
ρ, g/cm^3	1.858	1.865	1.719	1.783
μ, mm^{-1}	3.353	3.505	3.108	2.914
Crystal size, mm	0.22 × 0.20 × 0.15	0.30 × 0.25 × 0.22	0.12 × 0.08 × 0.05	0.3 × 0.20 × 0.18
θ_{max}, deg	29.00	25.99	26.00	28.65
Index range	$-15 \le h \le 15$, $-17 \le k \le 14$, $-18 \le l \le 18$	$-13 \le h \le 13$, $-15 \le k \le 15$, $-16 \le l \le 16$,	$-13 \le h \le 13$, $-15 \le k \le 14$, $-15 \le l \le 16$,	$-15 \le h \le 15$, $-16 \le k \le 16$, $-21 \le l \le 21$
Collected reflections	12442	13125	9976	21871
Independent reflections/R_{int}	7537/0.0287	5793/0.0209	5712/0.0320	10247/0.0504
Reflections with $I > 2\sigma(I)$	6911	5292	4083	6977
Refined parameters	374	389	373	493
Number of restraints on bond lengths	0	12	2	6
R_1, wR_2 ($I > 2\sigma(I)$)	0.0256, 0.0678	0.0238, 0.0667	0.0431, 0.0901	0.0486, 0.1017
R_1, wR_2 (all reflections)	0.0287, 0.0700	0.0272, 0.0692	0.0743, 0.1041	0.0921, 0.1199
Goodness-of-fit	1.025	0.989	0.981	0.945
$\Delta\rho_{max}/\Delta\rho_{min}$, e/Å^3	0.809/–1.051	0.712/–0.688	0.529/–0.521	1.186/–0.992

X-ray diffraction analysis. Experimental data of X-ray diffraction analyses for compounds **I**–**IV** were obtained on a Bruker SMART APEX2 diffractometer [18] (Table 1) (Center for Collective Use at the Kurnakov Institute of General and Inorganic Chemistry, Russian Academy of Sciences). An absorption correction was applied by the semiempirical method from equivalents using the SADABS program [19]. Structures **I** and **IV** were determined by a combination of a direct method and Fourier syntheses. The primary model for isostructural crystals of compounds **II** and **III** was taken from the data for **I**. Structures **I**–**III** contain disordered coordinated DMSO molecules, and the solvate CH_2Cl_2 molecule is disordered in structure **IV**. The site occupancies of the disordered positions were obtained by the isotropic refinement of the structures with fixed thermal parameters of the disordered atoms (U_{iso}= 0.08 Å^2) and were not refined in subsequent calculations. Restraints were imposed on the geometric parameters of the disordered molecules in structures **II**–**IV**. Hydrogen atoms were calculated from geometric concepts and refined in the riding

model. The structures were refined by full-matrix anisotropic–isotropic least squares. All calculations were performed using the SHELXS-97 and SHELXL-97 programs [20].

Additional data for structures **I–IV** were deposited with the Cambridge Crystallographic Data Centre (nos. 959719 (**I**), 959720 (**II**), 959721 (**III**), and 959722 (**IV**); deposit@ccdc.cam.ac.uk or http://www.ccdc.cam.ac.uk).

The thermal decomposition of complexes **I–IV** was studied by differential scanning calorimetry (DSC) and thermogravimetry (TG) on NETZSCH instruments. The TG analyses were carried out in flows of artificial air (O_2 20.8%, CH_4 < 0.0001%) (20 mL/min) and argon (Ar > 99.998%, O_2 < 0.0002%, N_2 < 0.001%, water vapor < 0.0003%, CH_4 < 0.0001%) (20 mL/min) on a TG 209 F1 instrument in alundum crucibles at a heating rate of 10°C/min. The composition of the gas phase was studied on a QMS 403C Aëolos mass spectrometric attachment under the TG conditions. The energy of ionizing electrons was 70 eV, and the maximum determined mass number (ratio of the mass of the ion to its charge Z) was 300 amu. The weight of the samples for TG was 0.5–3 mg. The DSC studies in flows of dried artificial air and argon were carried out on a DSC 204 F1 calorimeter in aluminum cells at a heating rate of 10°C/min. The weighed samples of the compounds were 1–4 mg. The temperature calibrations of a thermobalance and a calorimeter were carried out by the points of the phase transitions of standard substances (C_6H_{12}, Hg, KNO_3, In, Sn, Bi, CsCl, purity 99.99%) according to the ISO/CD 11357-1 standard. For TG and DSC experiments, samples were weighed on a SARTORIUS RESEARCH R 160P analytical balance with an accuracy of 1×10^{-2} mg. Data of thermal analyses were processed according to the ISO 11357-1, ISO 11357-2, ISO 11358, and ASTM E 1269-95 standards using the NETZSCH Proteus Thermal Analysis analytical package.

The X-ray diffraction analyses of the decomposition products were carried out using an FR-552 monochromator-chamber ($CuK_{\alpha 1}$ radiation) using germanium as an internal standard (X-ray patterns were measured on an IZA-2 comparator with an accuracy of ±0.01 mm) and a G670 Guinier chamber (HUBER) ($CuK_{\alpha 1}$ radiation).

RESULTS AND DISCUSSION

Crystalline ferrocenecaroxylates **I–III** were obtained by the reaction of ferrocenecarboxylic acid, KOH, and $Ln(NO_3)_3 \cdot 6H_2O$ (ratio 2 : 2 : 1) in methanol in the presence of DMSO followed by the extraction of the product with toluene (scheme). In the case of using gadolinium chloride instead of nitrate (component ratio 3 : 3 : 1) in a similar reaction, complex **IV** was isolated after the extraction of the product with a mixture of toluene and CH_2Cl_2.

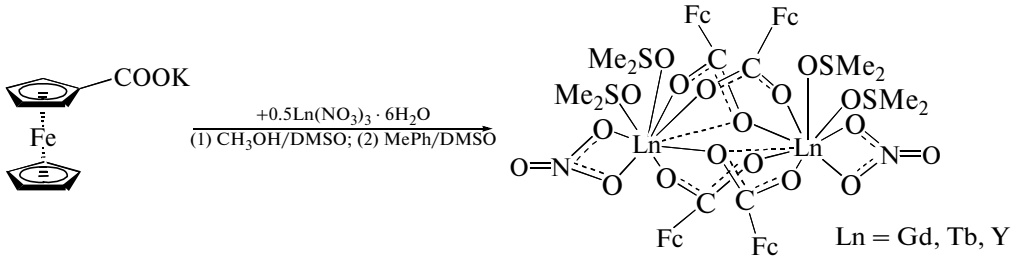

Scheme.

Structures **I–III** are formed by centrosymmetric dimers (Figs. 1a and 2, Table 2). Two Ln atoms are linked by two bridging and two chelate-bridging OOCFc ligands. The coordination mode of Ln is supplemented to ninefold by the NO_3^- chelating ion and two oxygen atoms of DMSO. Structure **IV** includes centrosymmetric dimers $[Gd_2(\mu\text{-}O,\eta^2\text{-}OOCFc)_2(\eta^2\text{-}OOCFc)_4(DMSO)_2(H_2O)_2]$ (Figs. 1b and 2) and solvate molecules DMSO and CH_2Cl_2. Among structures of binuclear lanthanide carboxylates, there are examples of analogs of both complexes **I–III** and **IV** [21]. We have earlier synthesized the binuclear rare-earth metal carboxylates containing the cymantrenyl fragment ($(\eta^5\text{-}C_5H_4)Mn(CO)_3$) similar in geometry to the ferrocenyl fragment. Rare-earth metal cymantrenecarboxylates are similar to complexes **I–III** [5, 22–24].

The Cambridge Structural Database (version 5.34, May 2013 [25]) contains the data about eleven Ln ferrocenecarboxylates: $[La_2(\mu\text{-}O,\eta^2\text{-}OOCFc)_2(\eta^2\text{-}OOCFc)_4(H_2O)_4] \cdot 2HOOCFc$ [26]; $[Ln_2(\mu\text{-}O,\eta^2\text{-}OOCFc)_2(\eta^2\text{-}OOCFc)_4(H_2O)_4] \cdot 2MeOH \cdot xH_2O$ (**V**), $x = 0$, Ln = Y [27] (MUTHUE); $x = 1$, Ln = La [28], Ce [29], Pr [30], Nd [27] (MUTHOY), Eu, Gd [28], Dy [15]; $[Gd_2(\mu\text{-}O,\eta^2\text{-}OOCFc)_2(\eta^2\text{-}OOCFc)_4(H_2O)_2(MeOH)_2] \cdot 2MeOH \cdot 2H_2O$ [27] (MUTHIS) and $[Er_2(\mu\text{-}O,\eta^2\text{-}OOCFc)_2(\eta^2\text{-}OOCFc)_2(OOCFc)_2(H_2O)(MeOH)_2] \cdot 2MeOH$ [30] (SAFKOB). All seven compounds **V** with $x = 1$ are isostructural with each other, and the similarity of the

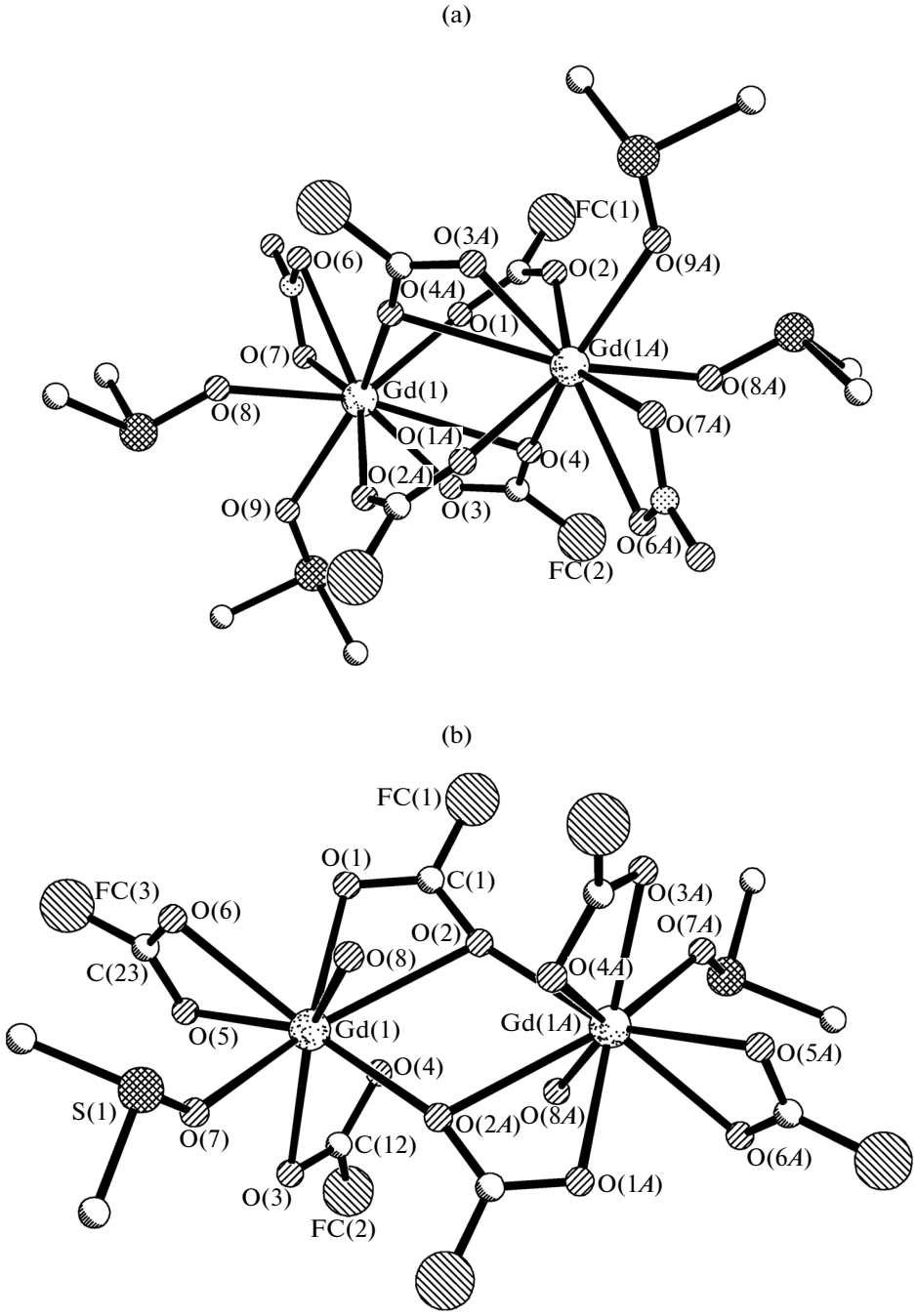

Fig. 1. Molecular structures of complexes (a) **I–III** and (b) **IV**, where FC is ferrocenyl.

crystal structure of yttrium compound MUTHUE ($x = 0$) makes it possible to consider it isostructural to these compounds. Ten of eleven complexes (except for SAFKOB) are similar to complex **IV** (taking into account the replacement of DMSO by H_2O or MeOH), and the coordination number of Ln is 9. In SAFKOB, one of the chelating OOCFc ligands is "transformed" into the monodentate one (the coordination number of Er is 8), and the uncoordinated oxygen atom of OOCFc is a hydrogen acceptor in the intramolecular hydrogen bond with the coordinated methanol molecule MeOH···O(OOCFc) (O···O 2.57 Å). Binuclear fragments can also be isolated in the structures of the derivatives of 1,1'-ferrocenedicarboxylic acid and rare-earth metals, which are coordination polymers. In all cases, the Ln^{3+} ions are linked by two chelate-bridging carboxylates [28, 31–33]. Thus, complexes **I–III** are the first examples of the rare-earth metal ferrocenecarboxylate complexes in

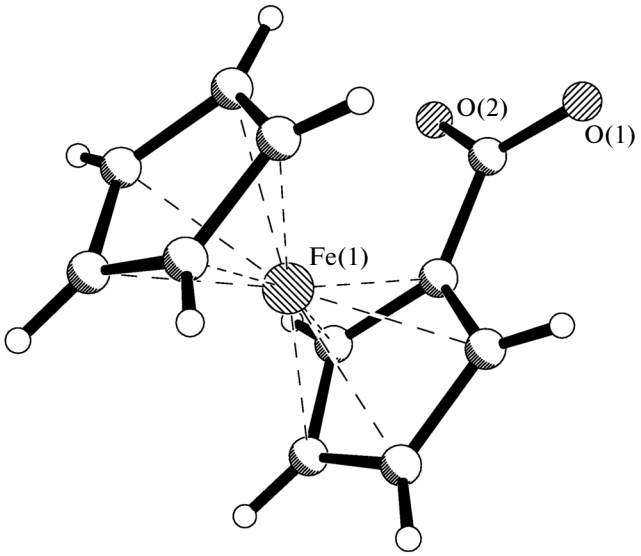

Fig. 2. Fragment Fe(CpCOO)(Cp) in structures **I–IV**.

which metal ions are linked by four carboxylate bridges.

The Nd, Gd, and Y complexes were synthesized under the same conditions [27], but the compositions of the structurally characterized complexes are different. Isostructural compounds MUTHOY and MUTHIS differ in hydrate composition, and one of the coordinated water molecules in SAFKOB is replaced by a methanol molecule. The structural diversity of compounds $[Ln_2(\mu\text{-}O,\eta^2\text{-}OOCFc)_2(\eta^2\text{-}OOCFc)_y(OOCFc)_{4-y}(H_2O)_z(MeOH)_{4-z}] \cdot 2MeOH \cdot xH_2O$ ($x = 0, 1, 2$; $y, z = 0, 2$) allows one to assume the existence of polymorphous and morphotropic transitions in these compounds similarly to that for $[Ln_2(\mu_2\text{-}OOCCym)_x(\mu\text{-}O,\eta^2\text{-}OOCCym)_{4-x}(\eta^2\text{-}NO_3)_2(\eta^2\text{-}MeOCH_2CH_2OMe)_2]$ ($x = 0, 2$) [5].

In complexes **I–III**, the Ln : Fe ratio is 1 : 2, which is close to the Ln : Fe ratio in ferrites with the garnet structure (3 : 5). Therefore, it was interesting to study the ability of complexes **I–III** to serve as precursors for garnet-like ferrites $Ln_3Fe_5O_{12}$ under the oxidative thermolysis conditions. The thermolysis of complexes **I–III** was studied in an atmosphere of argon and air. In both cases, the destruction process occurs in stages, and the main characteristics of the process are independent of the nature of the rare-earth metal ion. On heating in an argon flow, the primary mass loss (Table 3, Fig. 3) is accompanied by a pronounced endotherm, which is transformed into an exotherm at temperatures higher than ~200°C. An insignificant mass loss without noticeable energy changes in the system is observed above the temperature of the end of the first stage in the temperature range of about ~90°C. Then a considerable acceleration of the mass loss is observed (the second stage ranges from 80 to 100°C). A gradual mass loss accompanied by a broad endotherm is observed above the temperature of the end of the second stage. To reveal the mechanism of thermolysis in an inert atmosphere, we carried out the detailed TG study with the mass spectral analysis of the gas phase during thermal destruction for complex **III**.

We have earlier established the character of DMSO removal from rare-earth cymantrenecarboxylates [22]. It was shown that the removal of DMSO was

Table 2. M–O bond lengths and M···M' distances in structures **I–IV**

Bond	*d*, Å			
	I	**II**	**III**	**IV**
M(1)–O(1)	2.3755(18)	2.359(2)	2.330(3)	2.393(4)
M(1)–O(2)				2.828(4)
M(1)–O(2*A*)	2.3267(18)	2.307(2)	2.278(3)	2.370(4)
M(1)–O(3)	2.4030(19)	2.384(2)	2.352(3)	2.485(4)
M(1)–O(4)	2.922(2)	2.952(2)	3.023(3)	2.422(4)
M(1)–O(4*A*)	2.2938(18)	2.278(2)	2.244(3)	
M(1)–O(5)				2.386(4)
M(1)–O(6)	2.657(2)	2.649(3)	2.659(4)	2.543(4)
M(1)–O(7)	2.486(2)	2.466(2)	2.433(3)	2.397(3)
M(1)–O(8)	2.394(2)	2.377(2)	2.340(3)	2.415(4)
M(1)–O(9)	2.4080(19)	2.387(2)	2.360(3)	
M(1)···M(1*A*)	4.0669(2)	4.0671(3)	4.0881(8)	4.3482(7)

accompanied by the decomposition of the ligand. The gas phase contains both $(CH_3)_2SO$ and the products of its disproportionation, $(CH_3)_2S$ and $(CH_3)_2SO_2$. Under the TG conditions for complex **III**, the most characteristic ionic currents of the gas phase in the whole temperature range are presented in Fig. 4. The following peaks of ionic currents were detected in the mass spectrum of complex **III** in the temperature range 165–350°C: $[NO]^+$, $[(CH_3)_2SO_2]^+$, $[(CH_3)SO]^+$, $[(CH_3)_2S]^+$, and $[CH_3]^+$. This makes it possible to believe that the first stage includes the Y–$OS(CH_3)_2$ bond cleavage (bp (DMSO) = 189°C), ligand destruction, the onset of removal of the formed products (first endotherm), the intramolecular redox process involving nitrate ions, and the formation of some intermediate (exotherm). This assumption is confirmed by the TG results (Table 3). As can be seen from Fig. 4, both the partial removal of ferrocene (the ionic current peaks were detected in the mass spectrum above 380°C: $[(C_5H_5)Fe]^+$, $[Fe]^+$, and $[CO_2]^+$) and its destruction and the gradual formation of solid decomposition products occur at the second thermolysis stage. The thermolysis product in an inert atmosphere contains $Y_3Fe_5O_{12}$ and minor amounts of Fe_2O_3 (Table 4).

Table 3. Thermolysis characteristics of complexes **I**–**III**

Parameters	**I** (Gd)	**II** (Tb)	**III** (Y)
	in argon		
$T_{onset,\ 1\ st} \pm 2.0$, °C	188	173	165
$T_{end,\ 1\ st}$, °C	275	279	265
% DMSO + NO_3	26.4	26.3	28.7
% DMSO + NO	22.3	22.3	24.3
$\Delta m_{1\ st} \pm 1.5$, %	22.6	22.4	24.5
$T_{onset,\ 2\ st} \pm 2.0$, °C	390	395	380
$T_{end,\ 2\ st}$, °C	480	483	460
$\Delta m_{2\ st} \pm 2.0$, %	10.0	12.0	10.1
	In air flow		
$T_{onset,\ 1\ st} \pm 2.0$, °C	180	177	160
$T_{end,\ 1\ st} \pm 2.5$, °C	262	285	280
$\Delta m_{1\ st} \pm 1.5$, %	23.2	22.4	25.0
$T_{end} \pm 2.5$, °C	488	545	520

In the case of thermolysis of complexes **I**–**III** in air, the character of the first stage is similar to that of decomposition in argon (Table 3, Fig. 4). No considerable retardation of the mass loss is observed above 300°C. Evidently, the oxidative destruction of the molecule occurs and ceases to 500°C (the mass loss curve reaches a plateau). The single thermolysis product of the complexes in air, whose presence can be established by X-ray powder diffraction analysis (accuracy ±5 wt %) is ferrimagnetic garnet $Ln_3Fe_5O_{12}$ (Table 4). Further studies are needed to develop the procedure of obtaining preparative amounts of individual ferrites $Ln_3Fe_5O_{12}$ from ferrocenecarboxylates.

The magnetic properties of the lanthanide complexes are interesting and promising because of the high magnetic moment inherent to some Ln ions and the possibility of exchange interactions between them [34, 35]. The compounds containing the Gd^{3+} ion are especially interesting due to the electronic structure of this ion: it has the maximum possible number of unpaired electrons ($S = 7/2$) among the 4*f* elements.

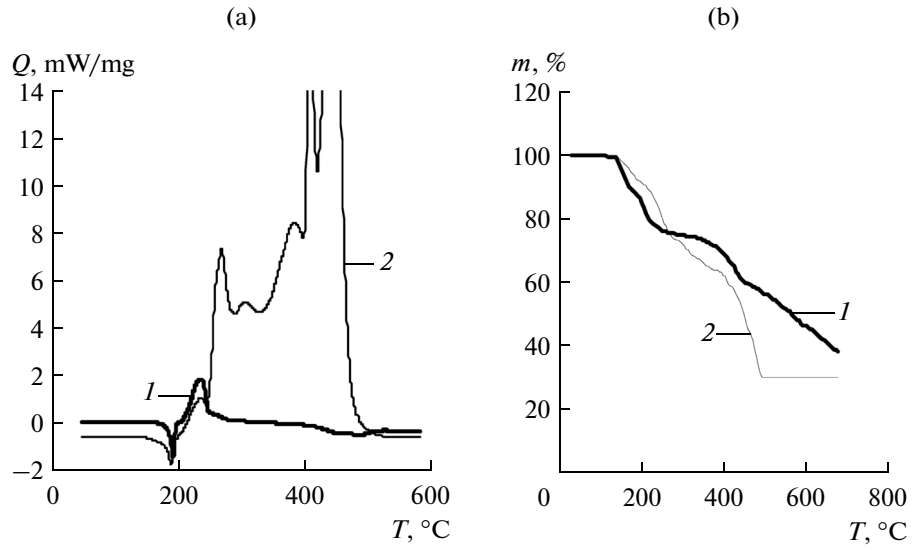

Fig. 3. (a) DSC curves and (b) the temperature dependence of the mass change for complex **III** in (*1*) argon and (*2*) air flow.

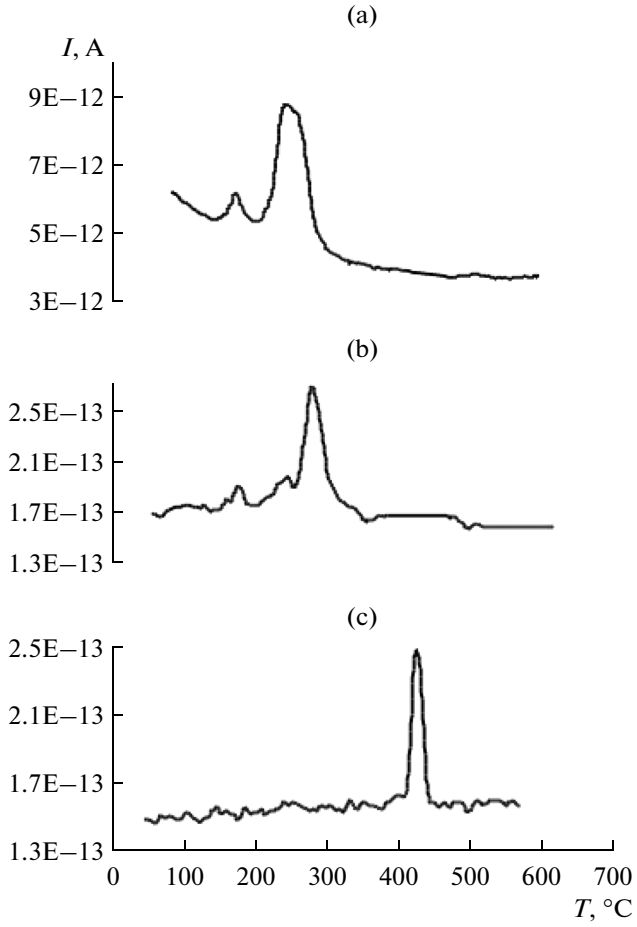

Fig. 4. Most characteristic ionic current in the mass spectrum of the gas phase under the thermogravimetric experiment conditions in argon for complex **III**: (a) $m/z = 30$ ($[NO]^+$), (b) $m/z = 15$ ($[CH_3]^+$), and (c) $m/z = 121$ ($[(C_5H_5)Fe]^+$).

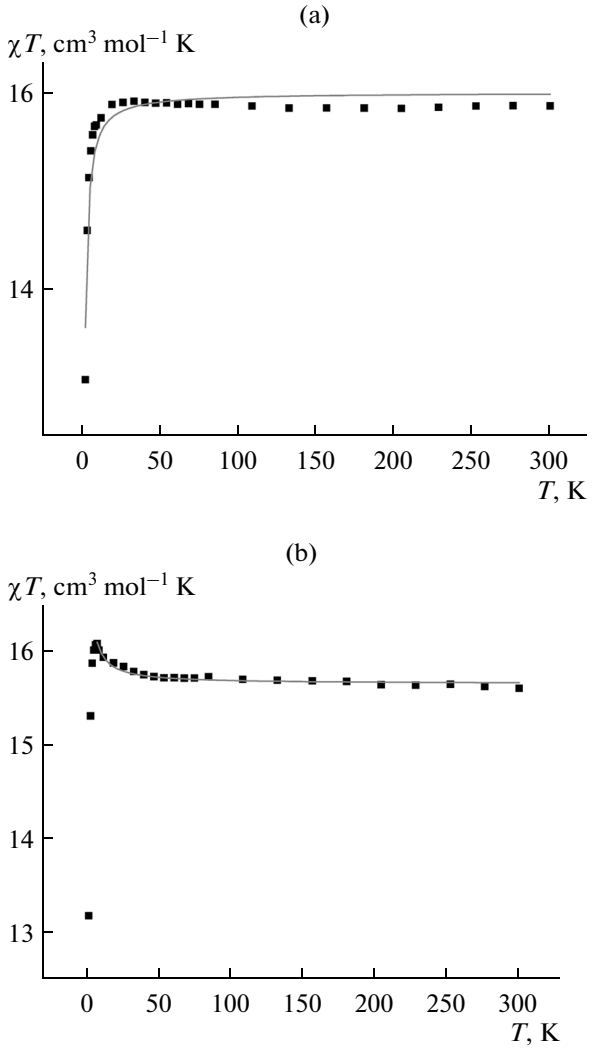

Fig. 5. Temperature dependences of $\chi_M T$ for complexes (a) **I** and (b) **IV**; (■) are experimental values, and (—) is calculated curve.

In addition, this is an isotropic ion, whose magnetic moment is determined by the spin component only, which facilitates the mathematical description of magnetism of the Gd^{3+} complexes. The temperature dependence of the magnetic susceptibility was studied for gadolinium complexes **I** and **IV**. For complex **I** at room temperature, the value of $\chi_M T$ is 15.87 $cm^3\ mol^{-1}\ K$, which is close to the calculated value (15.76 $cm^3\ mol^{-1}\ K$ [34]). As the temperature decreases, this value changes insignificantly down to 12 K, after which $\chi_M T$ decreases sharply (Fig. 5a). The temperature dependence of the inverse magnetic susceptibility $1/\chi$ for complex **I** is described by the Curie–Weiss law with constants $C = 15.8692 \pm 0.0052\ cm^3\ mol^{-1}\ K$ and $\theta = -0.06606 \pm 0.04165$ K. An analysis of the experimental data in terms of the formal model proposed [36] in the form of equations derived from the Hamiltonian at the isotropic spin and quantum number $S_{Gd} = S_{Gd'} = 7/2$ indicates the predomination of antiferromagnetic interactions in complex **I** with constant $J = -0.03984 \pm 0.00252\ cm^{-1}$ (at $g = 2.016$).

The behavior of another Gd-containing complex **IV** differs from that of complex **I**. A pronounced increase of $\chi_M T$ (from 15.58 to 16.06 $cm^3\ mol^{-1}\ K$) is observed with the temperature decrease in the almost whole studied range (300–7.83 K) followed by a sharper decrease than that observed in the first case. In the range of increasing $\chi_M T$, an analysis indicates the ferromagnetic exchange ($J = 0.02933 \pm 0.00146\ cm^{-1}$ at $g = 1.99$) (Fig. 5b). The dependence of $1/\chi$ on T in the range 300–9 K corresponds to the Curie–Weiss law with constants $C = 14.35269 \pm 0.00765\ cm^3\ mol^{-1}\ K$ and $\theta = 0.44966 \pm 0.07663$ K. The dependence of the spin exchange constant $J_{Gd–Gd'}$ on the interatomic spacing $D_{Gd\cdots Gd'}$ for the Gd complexes containing the binuclear $[Gd_2O_2]$ fragment with two bridging oxygen atoms was earlier established from the experimental data [37]. It was found that the antiferromagnetic interaction between the Gd^{3+} ions weakened with the elongation of the distance and changed to the ferro-

Table 4. Phase analysis of the solid decomposition products of complex **III**

Product				$Y_3Fe_5O_{12}$ [33-0507]*		Fe_2O_3 [79-1691]*	
in argon		in air					
d, Å	*I*, %	*d*, Å	*I*, %	*d*, Å	*I*, %	*d*, Å	*I*, %
5.0	10	5.0		5.0507	5		
3.09	40	3.09		3.0942	30		
2.77	100	2.77		2.768	100		
2.70	10					2.7140	100
2.53	80	2.53		2.5270	44		
						2.3500	16
2.26	20	2.26		2.2603	9		
						2.0050	10
1.79	30	1.79		1.7869	15		
1.715	40	1.715		1.7140	40		
1.65	80	1.65		1.6545	47	1.6620	40
1.543	30	1.543		1.5476	15		
						1.4170	19
1.38	10	1.38		1.3841	11		
1.35	30	1.35		1.3508	11		
1.32	10	1.32		1.3196	12	1.72	75
1.57	10			1.5681	16		

* Powder Diffraction File, Swarthmore: Joint Committee on Powder Diffraction Standards.

magnetic interaction at $D_{Gd\cdots Gd'}$ exceeding ~4.10 Å. For complex **I** and **IV**, $D_{Gd\cdots Gd'}$ is 4.0667 and 4.3482 Å, respectively. Thus, antiferromagnetic interactions in the first case and ferromagnetic interactions in the second case confirm the established correlation.

Thus, new heterometallic carboxylate 3*d*–4*f* complexes were synthesized in which the transition metal is bound to the aromatic π system, $[Ln_2(\mu\text{-}O,\eta^2\text{-}OOCFc)_2(\mu_2\text{-}O,O'\text{-}OOCFc)_2(\eta^2\text{-}NO_3)_2(DMSO)_4]$ (Ln = Gd (**I**), Tb (**II**), and Y (**III**)). The binuclear structure of the complexes includes four bridging carboxylates, two of which are chelate-bridging. Such structure has been found for the first time for rare-earth metal ferrocenecarboxylates. Complex $[Gd_2(\mu\text{-}O,\eta^2\text{-}OOCFc)_2(\eta^2\text{-}OOCFc)_4(DMSO)_2(H_2O)_2]\cdot 2DMSO\cdot 2CH_2Cl_2$ (**IV**) was obtained using gadolinium chloride under similar conditions. This complex has the binuclear structure with two chelate-bridging carboxylates typical of lanthanide ferrocenecarboxylates. The thermal decomposition of complexes **I**–**III** was shown to proceed similarly and to have the staged character. The thermolysis products of the complexes contain garnets $Ln_3Fe_5O_{12}$. It is shown that rare-earth metal ferrocenecarboxylates can serve as precursors for lanthanide–iron garnets that are valuable magnetic materials [38]. The magnetic behavior of complexes **I** and **IV** was studied in the range from room to helium temperatures. The weak antiferromagnetic interaction

between the Gd ions was found in the first case, whereas this interaction is weak ferromagnetic in the second case.

ACKNOWLEDGMENTS

This work was supported by the Russian Foundation for Basic Research (project nos. 13-03-12428, 14-03-00463, and 14-03-00470), the Council on Grants at the President of the Russian Federation (program for state support of leading scientific schools NSh-1712.2014.3), the President of the Russian Federation (scholarship SP-6585.2013.5), and the Presidium of the Russian Academy of Sciences.

REFERENCES

1. Singha, M.K., Yanga, Y., and Takoudis, Ch.G., *Coord. Chem. Rev.,* 2009, vol. 253, p. 2920.
2. Revaprasadu, N. and Mlondo, S.N., *Pure Appl. Chem.*, 2006, vol. 78, no. 9, p. 1691.
3. Kaul', A.R., Gorbenko, O.Yu., and Kamenev, A.A., *Usp. Khim.,* 2004, vol. 73, p. 932.
4. Vertoprakhov, V.N., Nikulina, L.D., and Igumenov, I.K., *Usp. Khim.,* 2005, vol. 74, p. 797.
5. Koroteev, P.S., Dobrokhotova, Zh.V., Ilyukhin, A.B., et al., *Polyhedron,* 2013, vol. 65, p. 110.
6. Sakamoto, M., Manseki, K., and Okawa, H., *Coord. Chem. Rev.*, 2001, vols. 219–221, p. 379.
7. Winpenny, R.E.P., *Chem. Soc. Rev.*, 1998, vol. 27, p. 447.
8. Andruh, M., Costes, J.-P., Diaz, C., and Gao, S., *Inorg. Chem.*, 2009, vol. 48, p. 3342.
9. Huang You-Gui, Jiang Fei-Long, and Hong Mao-Chun, *Coord. Chem. Rev.*, 2009, vol. 253, p. 2814.
10. Cullen, W.R. and Woollins, J.D., *Coord. Chem. Rev.*, 1981, vol. 39, p. 1.
11. Gaponik, P.I., Lesnikovich, A.I., and Orlik, Yu.G., *Usp. Khim.*, 1983, vol. 52, p. 294.
12. Hou Hongwei, Li Linke, *Leading Edge Organomet. Chem. Res.*, 2006, p. 27.
13. Li Lin-Ke, Cao Zhen-Yu, and Hou Hong-Wei, *J. Coord. Chem.*, 2008, vol. 61, p. 2105.
14. Mereacre, V., Ako Ayuk, M., Filoti, G., et al., *Polyhedron*, 2010, vol. 29, p. 244.
15. Liu, J., Li, Y., and Li, D., *Acta Crystallogr., Sect. E: Structure Reports Online*, 2012, vol. 68, p. m6.
16. Yan, P.F., Zhang, F.M., Li, G.M., et al., *J. Solid State Chem.*, 2009, vol. 182, p. 1685.
17. Li Linke, Li Jinpeng, Hou Hongwei, et al., *Inorg. Chim. Acta*, 2006, vol. 359, p. 3139.
18. *APEX2 and SAINT*, Madison (WI, USA): Bruker AXS Inc., 2007.
19. Sheldrick, G.M., *SADABS*, Göttingen (Germany): Univ. of Göttingen, 1997.
20. Sheldrick, G.M., *Acta Crystallogr., Sect. A: Found. Crystallogr.*, 2008, vol. 64, no. 1, p. 112.
21. Huang, Ch., *Rare Earth Coordination Chemistry: Fundamentals and Applications*, Singapore: Wiley, 2010.
22. Koroteev, P.S., Dobrokhotova, Zh.V., Ilyukhin, A.B., et al., *Izv. Akad. Nauk., Ser. Khim.*, 2012, no. 6, p. 1064. (Russ. Chem. Bull., Int. Ed., 2012, vol. 61, no. 6, p. 1069).
23. Koroteev, P.S., Dobrokhotova, Zh.V., Kiskin, M.A., et al., *Polyhedron*, 2012, vol. 43, p. 36.
24. Koroteev, P.S., Kiskin, M.A., Dobrokhotova, Zh.V., et al., *Polyhedron*, 2011, vol. 30, p. 2523.
25. Allen, F.H., *Acta Crystallogr., Sect. B: Struct. Sci.*, 2002, vol. 58, no. 3, p. 380.
26. Li Gang, Hou Hongwei, Li Linke, et al., *Acta Chim. Sin.*, 2004, vol. 62, no. 11, p. 1060.
27. Hou Hongwei, Li Gang, Li Linke et al., *Inorg. Chem.*, 2003, vol. 42, p. 428.
28. Dong Guo, Yu-Ting Li, Chun-Ying Duan, et al., *Inorg. Chem.*, 2003, vol. 42, p. 2519.
29. Wen, L., Zhang, B., Peng, Z., et al., *Chin. J. Inorg. Chem.*, 2004, vol. 20, no. 10, p. 1228.
30. Jiang, L.-P., Cai, Y.-L., Liang, F.-P., et al., *J. Guangxi Normal Univ. (Nat. Sci. Edition)*, 2009, no. 1, p. 59.
31. Yang Yang-Yi and Wong Wing-Tak, *Chem. Commun.*, 2002, p. 2716.
32. Meng Xiangru, Li Gang, Hou Hongwei, et al., *J. Organomet. Chem.*, 2003, vol. 679, p.153.
33. Dong Guo, Bing-guang Zhang, Chun-ying Duan, et al., *Dalton Trans.*, 2003, p. 282.
34. Benelli, C. and Gatteschi, D., *Chem. Rev.*, 2002, vol. 102, p. 2369.
35. Wang Bing Wu, Jiang Shang Da, Wang Xiu Teng, and Gao Song, *Sci. China. B.*, 2009, vol. 52, p. 1739.
36. Panagiotopoulos, A., Zafiropoulos, T.F., Perlepes, S.P., et al., *Inorg. Chem.*, 1995, vol. 34.
37. Koroteev, P.S., Efimov, N.N., Dobrokhotova, Zh.V., et al., *Izv. Akad. Nauk., Ser. Khim.*, 2013, no 8, p. 1768 (Russ. Chem. Bull., Int. Ed., 2013, vol. 62, no. 8, p. 1768).
38. Baek Kim Sung, Je Moon Seung, Jin Kim Sam, Sung Kim Chul, *J. Magn. Magn. Mat.*, 2007, vol. 310, p. e592.

Translated by E. Yablonskaya